Int J Adv Manuf Technol (2018) 94:523–532
DOI 10.1007/s00170-017-0859-z

ORIGINAL ARTICLE

An adaptive repair surface modeling approach for worn blades

Feiru Hou[1] · **Neng Wan**[1] · **Zhiyong Chang**[1] · **Zezhong Chen**[1,2] · **Huibin Sun**[1]

Received: 6 April 2017 / Accepted: 20 July 2017 / Published online: 12 August 2017

Abstract Currently, worn blade repair work, obtaining the target surfaces manually wastes too much time. To improve repair ability, an innovative adaptive repair strategy is proposed which covers pre-inspection, welding, and machining process. Different from finding repairing surface manually, the welded surface and machining surface are restructured with less manual intervention. The welded surface ensured enough material for subsequent machining is captured by extracting upper profile boundary surface of its design one. Furthermore, a target machining surface satisfied design requirements, machining allowance, and geometric continuity is restructured using an effective optimization method. To prove the availability of the proposed method in this paper, a compressor blade repair instance, including welded surface and machining surface optimization and simulation is demonstrated at last.

Keywords Adaptive repairing · Profile tolerance · Shape optimization · Geometric continuity

1 Introduction

The vane made of superalloy material is a kind of core component for gas turbine engines and can be mainly divided into two categories, such as compressor blades and turbine blades. Due to the severe working environment, these blades are easy to be worn caused by high temperature, high pressure gas, or centrifugal forces [1, 2]. Influenced by the defect, worn blades would lose their function. However, the complex manufacturing process and special difficult-to-machine material make blade particularly expensive. Many companies would repair blade instead of replacing a new one in view of economy. Therefore, achieving an adaptive high-precision blade repair is of great significance.

In general, repairing worn blades starts from removal of material on worn area. And then, laser welding technology is used to fill material in the corresponding area. Finally, an adaptive machining solution is utilized to cut back to ensure final design shape [3, 4]. Due to the extensive work, the shape of the worn blade is not exactly the same as the design's. Therefore, the design surface cannot be fully used to plan the tool path during the repair process. Moreover, a blade's shape has high-precision requirements. Even a small deviation of the shape for the machining surface may lead to a large influence on the gas turbine engines performance [5, 6]. Therefore, it is very important to capture the target machining surface of the worn blade, control its shape to yield tolerance requirement, and ensure geometric continuity with the undamaged area adaptively.

2 Literature review

In recent years, repairing blades is a research hotspot with the rapid growth of aviation industries. The kernel point is to create suitable target surfaces which play a crucial role for the tool path generation in the welding process and machining process. Current studies can be classified into two approaches: (1) the machining surface is constructed from the whole or a part of design surface directly and (2) the machining surface is

✉ Feiru Hou
tina1sg@mail.nwpu.edu.cn; houfeiruyy@163.com

[1] Department of Mechanical Engineering, Northwestern Polytechnical University, Xi'an, Shaanxi 710072, China

[2] Department of Mechanical and Industrial Engineering, Concordia University, Montreal, Quebec H3G 1m8, Canada

constructed manually based on the measured model of worn blade. Bremer [7] presented a method of repairing straight blades, whose welded surface was obtained by fitting surface with a group of scattered points in reverse engineering software. Finally, the tool path was adjusted through comparing welded surface and design surface. Subsequently, an automated blade repair robot polishing system was researched [8, 9], and it was mainly used for machining operations. Similarly, design surface was adopted as the machining surface. Difference from machining of all blade body in above researches, the worn area, recognized by comparing the service blade and design surface, and was reconstructed in triangular mesh [10]. However, the accuracy of machining surface is decreased with triangular mesh. In these researches, the design surface is utilized as the target machining surface of worn blade in to-be-repaired area.

In fact, due to long time of work, the real shape of worn blade differs significantly from the design surface's. Therefore, it is inappropriate to use the design surface directly as the target machining surface. Brinksmeier [11] put forward a new method that the machining surface was obtained by comparing the welded surface and its corresponding master blade. However, the machining surface, determined manually, needs to adjust frequently once it deviates tolerance requirement. Bryan [12] proposed a profile algorithm to revise blade tip's shape. The machining surface was reconstructed based on the geometry comparison of neutral lines of design blade and service blade in worn area. Subsequently, an adaptive repair expert system [13, 14] including various master models and corresponding repair strategies was proposed. However, the expert system is difficult to suit for all blades owing to the differences in shape of each worn blade. In practice, a complete worn blade surface is usually composed by repaired area and unrepaired area. In order to obtain a high-accuracy machining surface satisfied its design requirements. He [15] proposed a method that reconstructed the part in worn area based on a CAD system; the geometric constraints were integrated into the fitting process. An automatic blade repair technology integrated with pre-repair inspection, build-up process, adaptive machining process, and post-repair inspection was introduced [16–20]. In which a high-quality master model was created according to a cloud of measured points, then the worn blade surface was aligned with the master model to capture target machining surface. Later, a similar repair method was proposed [21]. The welded blade tip was reconstructed adaptively considering the geometric characteristics. Zhang [22] maintained a geometry reconstruction approach based on cross-section curves blending with wavelet decomposition for adaptive blade repair.

Although the above researches are direct and clear. There still exist some issues as follows: (1) Due to the deformation of the worn blade, it is not appropriate to use the design surface to be the machining surface in worn area. (2) The method experience based on finding target machining surface relies on manual work and costs too much time. (3) To obtain the machining surface satisfied the design tolerance, the adjustment process cannot be avoided. However, this paper will focus on developing an adaptive solution to reconstruct target surfaces of both welding process and machining process based on measured model, which can meet the design requirements and avoid frequent manual adjustments.

The remainder of the paper is organized as follows: three important surfaces are described in Section 3. The welded surface ensured enough material for subsequent machining is presented in Section 4. Based on the free-form deformation transformation of the profile curves, reconstructing machining surface is discussed in Section 5. In Section 6, a simulation is used to verify the proposed method. Conclusions are given in Section 7.

3 Defining three type surfaces

Design surface from a designer is the CAD model and denoted as $\mathbf{S}^{\mathrm{D}}(u, v)$. The shape of design surface is controlled by a group of section curves paralleling to the *XOY* plane (Fig. 1a). Profile tolerances are defined on these sections to control blade's shape. For example, the tolerances of the pressure surface and suction surface is R_y, and which of the leading and trailing area is R_q and R_h (Fig. 1b).

A blade repair process includes regularizing worn area, increasing material on to-be-repaired area, and machining back to restore its original shape. In regularization process, irregular worn area is cut into a regular area owing to unavailable parametric surface representation (Fig. 2a, Fig. 2b). Then, a tool path for welding process is generated based on the well-created regular surface. Once the welding process is finished, the adaptive machining process is performed to remove excess material to restore its original expected shape.

Welded surface is the target surface of the increasing material process and denoted as $\mathbf{S}^{\mathrm{W}}(u, v)$. The welded surface is constructed based on regularized blade and also needs to provide enough material for subsequent machining (Fig. 2c).

Machining surface is the target surface of the finish machining and denoted as $\mathbf{S}^{\mathrm{M}}(u, v)$. Design tolerance and geometric continuity need to be yielded (Fig. 2d).

Before repairing, the worn blade is clamped on a machine, when the machining datum and design datum align were finished. If the deviation between the measured points of worn surface and design surface is not out of profile tolerance zone, then the worn area can be cut into regular area with determined parameter field. Otherwise, the blade may be considered to be scrapped. The process is called pre-inspection.

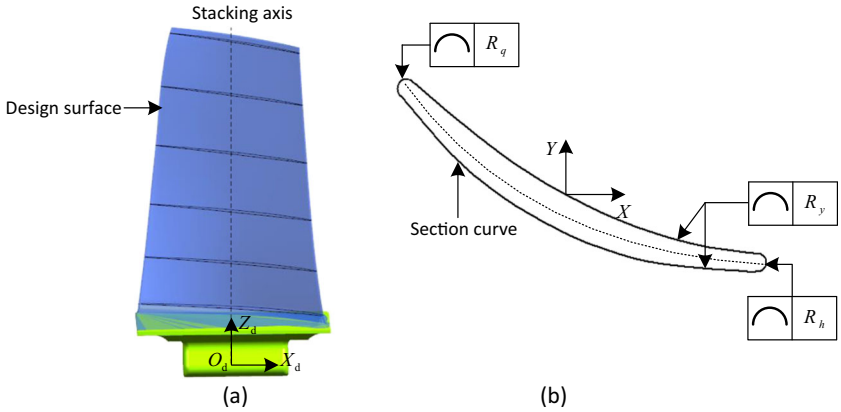

Fig. 1 Design model of the blade. **a** Design surface. **b** Profile tolerance of section curve

4 Welded surface modeling

Creating a welded surface modeling requires a regular parameter field $[u_a, u_b]$ and $[v_a, v_b]$. For regular cut blade, two sets of measured points $P_A = \{p_{1,i}, p_{2,i}, \ldots, p_{n,i}\}, i = 1, 2, \cdots, N$ and $P_B = \{p_{1,j}, p_{2,j}, \ldots, p_{n,j}\}, j = 1, 2, \cdots, N$, corresponding to area A and area B are selected out using three coordinate measuring machine (Fig. 3a). In the u direction, the section curves, denoted as $\mathbf{C}^{\mathsf{u}}(u) = \left\{\mathbf{c}_1^{\mathsf{u}}(u), \mathbf{c}_2^{\mathsf{u}}(u), \ldots, \mathbf{c}_n^{\mathsf{u}}(u)\right\}$, are fitted from each row measured points with same v parameter on area A. Similarly, the section curves, denoted as $\mathbf{C}^{\mathsf{v}}(v) = \left\{\mathbf{c}_1^{\mathsf{v}}(v), \mathbf{c}_2^{\mathsf{v}}(v), \ldots, \mathbf{c}_n^{\mathsf{v}}(v)\right\}$, are fitted from each column measured points with same u parameter on area B.

As the definition of design surface, profile tolerance is defined at design section curves. The upper profile tolerance curves are shown in (Fig. 3b). According to the surface reconstructed method, the profile tolerance surface $\mathbf{S}^{\mathsf{U}}(u, v)$ is lofted by upper profile tolerance curves [23] (Fig. 3c).

The v parameter of each row of measured points P_A is the same, and the $z$coordinate value is denoted as $p_{n,i}(z)$. The average z value of measured points in $n$row is the following:

$$z_n^A = \sum_{i=1}^{N} p_{n,i}(z)/N \tag{1}$$

A series of planes paralleling to XOY plane is built up at each z_n^A which is denoted as $\{H_1, H_2, \cdots, H_n\}$ (Fig. 4a). The intersection curves $\mathbf{C}^{\mathsf{U}}(u) = \left\{\mathbf{c}_1^{\mathsf{U}}(u), \mathbf{c}_2^{\mathsf{U}}(u), \cdots, \mathbf{c}_n^{\mathsf{U}}(u)\right\}$ between $\mathbf{S}^{\mathsf{U}}(u, v)$ and these planes are obtained by Newton iterative method [24] (Fig. 4b).

According to the parameter range $[u_a, u_b]$ of damaged area, a partitioning algorithm [25] is used to capture the curve segments $\overline{\mathbf{C}}^{\mathsf{U}}(u) = \left\{\overline{\mathbf{c}}_1{}^{\mathsf{U}}(u), \overline{\mathbf{c}}_2{}^{\mathsf{U}}(u), \cdots, \overline{\mathbf{c}}_n{}^{\mathsf{U}}(u)\right\}$ of the repaired area (Fig. 5a). In this way, a series of curves is created which can eventually replicates the 3D welded surface from the geometric model of the worn area. Then, the welded surface is restructured by lofting these curves $\mathbf{S}^{\mathsf{W}}(u, v) = skin\left(\overline{\mathbf{C}}^{\mathsf{U}}(u)\right)$ (Fig. 5b).

5 Machining surface modeling

A common issue encountered is that the design surface is different from its worn one and thus not suitable for taking as the target machining surface directly. Therefore, a machining surface satisfied boundary geometric continuities and profile tolerance requirement is created to best-fit the remaining blade area.

The machining surface would be restructured by optimizing the shape of design cross-section curves. The parameter field of blade to-be-repaired area on design surface is $[u_a, u_b]$ and $[v_a, v_b]$. Similar method to calculate the intersection

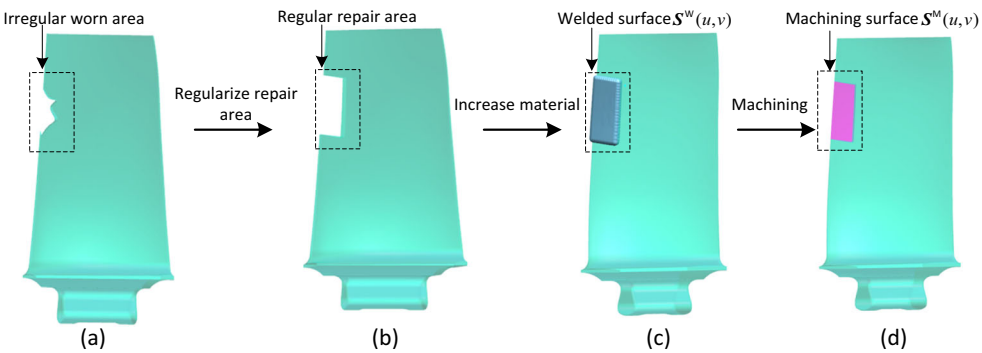

Fig. 2 Blade repair process. **a** The worn blade. **b** Regular area of to-be-repaired blade. **c** The welded surface. **d** The machining surface

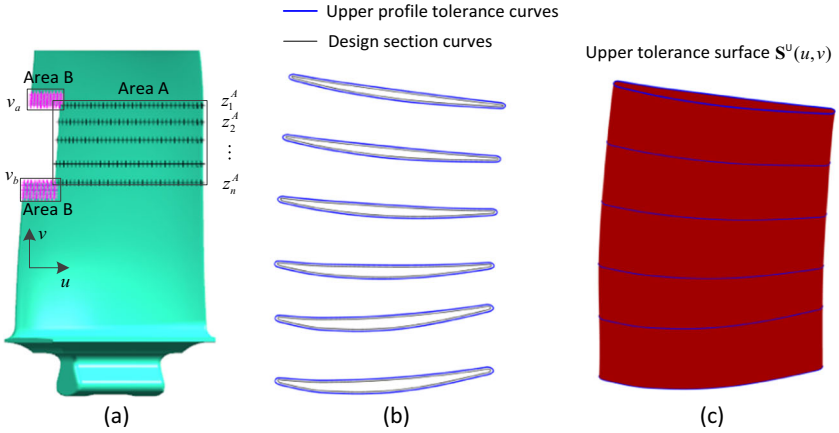

Fig. 3 The process of obtaining upper tolerance boundary surface. **a** Measured points of to-be-repaired blade. **b** Upper profile tolerance boundary curves. **c** Upper tolerance boundary surface

curves between $\mathbf{S}^{\mathrm{D}}(u,v)$ and $\{H_1, H_2, \cdots, H_n\}$, then the partitioning algorithm is used to capture the curve segments $\mathbf{C}^{\mathrm{D}}(u) = \left\{\mathbf{c}_1^{\mathrm{D}}(u), \mathbf{c}_2^{\mathrm{D}}(u), \ldots, \mathbf{c}_n^{\mathrm{D}}(u)\right\}$ of the repaired area.

Each curve $\mathbf{c}_j^{\mathrm{D}}(u), j = 1, 2, \cdots, n$ is defined as the following:

$$\mathbf{c}_j^{\mathrm{D}}(u) = \sum_{i=0}^{m} N_{i,3}(u) \cdot \mathbf{V}_{i,j} \quad u_a \le u \le u_b \tag{2}$$

where $N_{i,3}(u)$ is the basis function of cubic B-spline curve $\mathbf{c}_j^{\mathrm{D}}(u)$ with $m+1$ control points $\mathbf{V}_{i,j}$.

The section curve, denoted as $\tilde{\mathbf{c}}_j^{\mathrm{D}}(u)$ which is on machining surface and deformed from $\mathbf{c}_j^{\mathrm{D}}(u)$, which can be described as the following:

$$\tilde{\mathbf{c}}_j^{\mathrm{D}}(u) = \sum_{i=0}^{m} N_{i,3}(u) \cdot \left(\mathbf{V}_{i,j} \cdot \mathbf{R}_j + \Delta\mathbf{V}_{i,j}\right) \quad u_a \le u \le u_b \tag{3}$$

where $\mathbf{R}_j$ is the rotation matrix around the stacking axis, $\Delta\mathbf{V}_{i,j}$ is the control points' displacement in the plane H_j. The machining surface $\mathbf{S}^{\mathrm{M}}(u,v)$ is constructed by lofting curves $\tilde{\mathbf{c}}_j^{\mathrm{D}}(u), j = 1, 2, \cdots, n$ and denoted as $\mathbf{S}^{\mathrm{M}}(u,v) = skin\left(\tilde{\mathbf{C}}^{\mathrm{D}}(u)\right)$. Therefore, the key to obtain an applicable target machining surface is to get suitable parameter $\mathbf{R}_j$ and $\Delta\mathbf{V}_{i,j}$.

Based on an effective optimization method, an adaptive approach combining multi-objective and multi-constraint is presented for development of high-precision target machining surface.

5.1 Objective function

The machining surface is a part of to-be-repaired surface. It is hoped that the deformation between machining surface and its corresponding design area is as small as possible. Besides, the welded surface is the blank of the machining surface, it expects the machining surface has a uniform cutting allowance. The first objective function:

$$\min\left(g\left(\mathbf{R}_j, \Delta\mathbf{V}_{i,j}\right)\right) = \min\left(\int_0^1 \left\|k_j - k_i\right\|_2^2 ds\right) \tag{4}$$

where k_j and k_i are the curvature of scatter points on machining surface and isoparametric points on design surface, ds is arc length differential.

The second objective function:

$$\min\left(h\left(\mathbf{R}_j, \Delta\mathbf{V}_{i,j}\right)\right) = \min\left(\sum_{i=1}^{N_1} \left\|\mathbf{p}_i - \mathbf{q}_i\right\|^2\right) \tag{5}$$

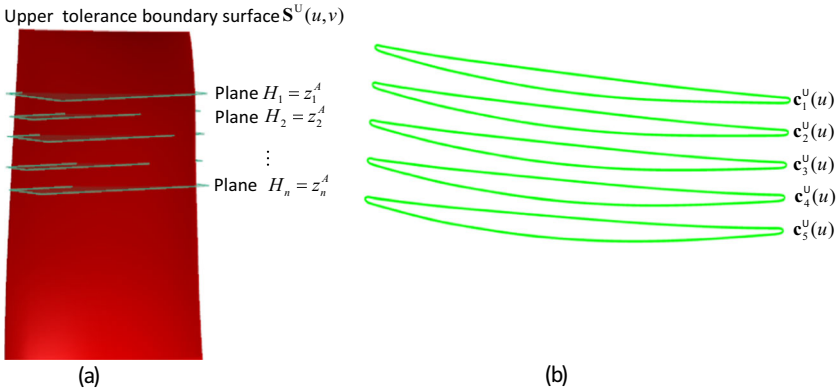

Fig. 4 Intersection curves of the repaired area. **a** The planes of specific height. **b** Intersection curves

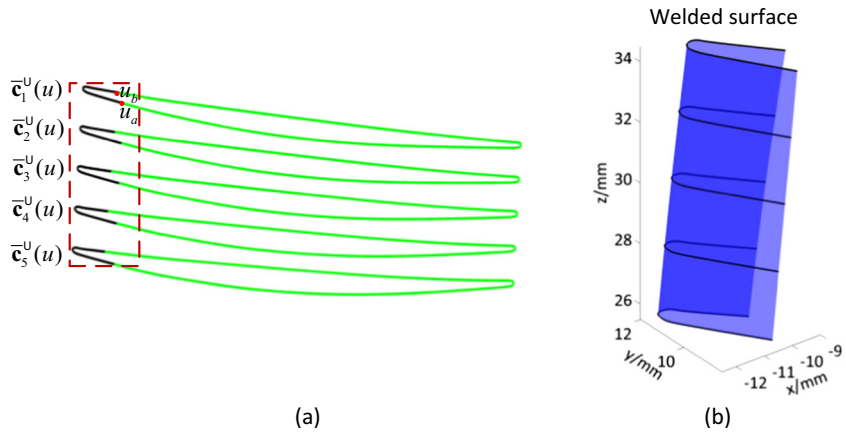

Fig. 5 Solving process of the welded surface. **a** The curves of the repaired area. **b** The welded surface

where $\mathbf{p}_i$ is the measured point of welded surface, and $\mathbf{q}_i$ is the nearest point on$\mathbf{S}^{\mathrm{M}}(u,v)$ corresponding to $\mathbf{p}_i$ (Fig. 6), N_1 is the number of measured points.

5.2 Tolerance constraint

The shape of the blade is crucial to the performance of the gas turbine engine. Therefore, as the basis of NC programming, the machining surface cannot be out of profile tolerance. The tolerance constraint is built up as follows:

$$sign\cdot(\mathbf{e}_i-\mathbf{q}_i)\cdot\mathbf{n}_i\geq 0,\quad i=1,2,\cdots,N_1 \tag{6}$$

The points set denoted as $\mathbf{e}_i$ is the scattered points of profile tolerance surface, $\mathbf{q}_i$ is the nearest points on the machining surface corresponding to $\mathbf{e}_i$, and $\mathbf{n}_i$ is the unit outer normal vector. If $\mathbf{e}_i$ is the points scattered from the upper profile tolerance boundary, then the sign = 1. If $\mathbf{e}_i$ is the points scattered from the lower profile tolerance boundary, the sign = − 1.

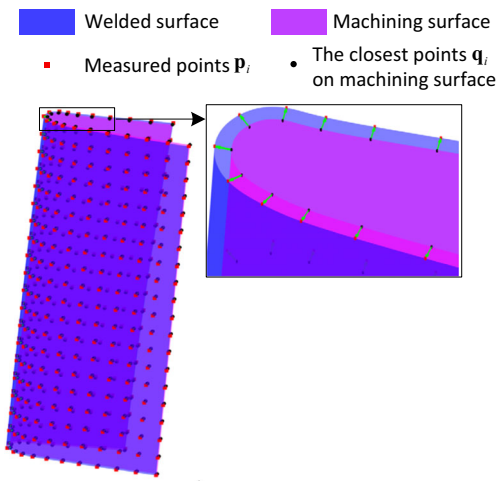

Fig. 6 The closest points from the measured points to the machining surface

5.3 Machining allowance constraint

The machining allowance is essential for finish machining area, and its constraint is built up as follows:

$$(\mathbf{p}_i-\mathbf{q}_i)\cdot\mathbf{n}_i\geq 0,\quad i=1,2,\cdots,N_1 \tag{7}$$

5.4 Continuity constraint

The boundary geometric continuities require that the target machining surface and the undamaged surface remain the continuity of position and first order tangent in the$u$, v direction, respectively. In addition, the continuity of the second order tangent is also guaranteed in the u direction. The section curve $\tilde{\mathbf{c}}_j^{\mathrm{D}}(u)$ of machining surface should keep continuous with the curve $\mathbf{c}_j^{\mathrm{u}}(u)$.

$$\tilde{\mathbf{c}}_j^{\mathrm{D}}(u_a)-\mathbf{c}_j^{\mathrm{u}}(0)=\mathbf{0},\quad \tilde{\mathbf{c}}_j^{\mathrm{D}}(u_b)-\mathbf{c}_j^{\mathrm{u}}(1)=\mathbf{0},\quad j=1,2,\cdots,n \tag{8}$$

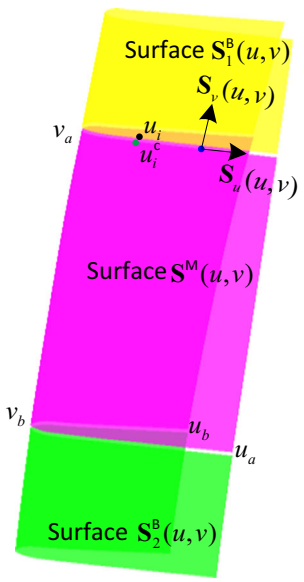

Fig. 7 Continuity of the machining surface in the v direction

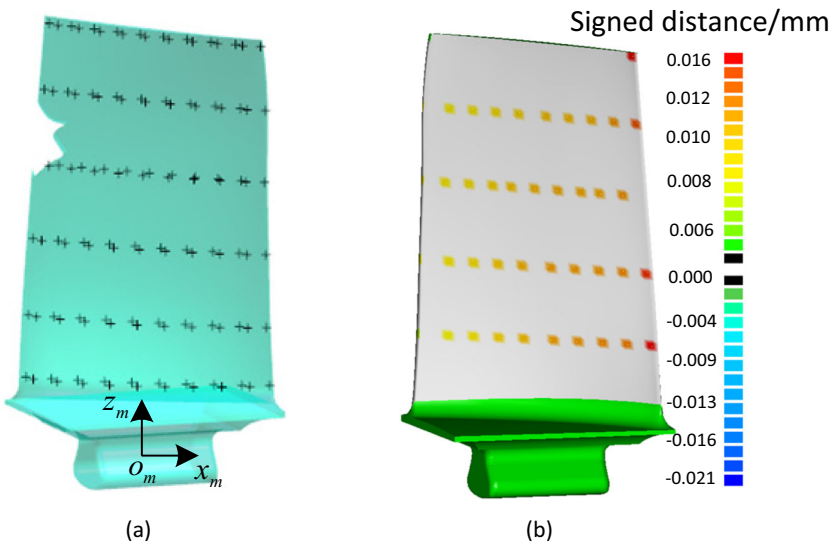

Fig. 8 Inspecting the damaged blade whether can be repaired. **a** Measured points of the service blade. **b** Signed distance from the measured points to design surface

$$\frac{\partial\left[\tilde{\mathbf{c}}_j^{\mathrm{D}}(u_a)\right]}{\partial u}-\frac{\partial\left[\mathbf{c}_j^{\mathrm{u}}(0)\right]}{\partial u}=\mathbf{0},\quad \frac{\partial\left[\tilde{\mathbf{c}}_j^{\mathrm{D}}(u_b)\right]}{\partial u}-\frac{\partial\left[\mathbf{c}_j^{\mathrm{u}}(1)\right]}{\partial u}=\mathbf{0},\quad j=1,2,\cdots,n \tag{9}$$

$$\frac{\partial^2\left[\tilde{\mathbf{c}}_j^{\mathrm{D}}(u_a)\right]}{\partial u^2}-\frac{\partial^2\left[\mathbf{c}_j^{\mathrm{u}}(0)\right]}{\partial u^2}=\mathbf{0},\quad \frac{\partial^2\left[\tilde{\mathbf{c}}_j^{\mathrm{D}}(u_b)\right]}{\partial u^2}-\frac{\partial^2\left[\mathbf{c}_j^{\mathrm{u}}(1)\right]}{\partial u^2}=\mathbf{0},\quad j=1,2,\cdots,n \tag{10}$$

Expressions (8), (9), and (10) are represented to constrain the boundary position continuity between the machined surface and the remaining surface, the boundary continuity of the first tangent, and the continuity of the second tangent in the u direction. $\frac{\partial(\mathbf{c}(u))}{\partial u}$ and $\frac{\partial^2(\mathbf{c}(u))}{\partial u^2}$ represent the first derivative and second derivative of the curve $\mathbf{c}(u)$ in the u direction, respectively.

The measured points of area B are fitted into a surface denoted as $\mathbf{S}_1^{\mathrm{B}}(u,v)$ and $\mathbf{S}_2^{\mathrm{B}}(u,v)$ (Fig. 7). The boundary geometric continuities between $\mathbf{S}^{\mathrm{M}}(u,v)$ and $\mathbf{S}^{\mathrm{B}}(u,v)$ need to be kept in the v direction.

$$\mathbf{S}_1^{\mathrm{B}}(u_i,0)-\mathbf{S}^{\mathrm{M}}\left(u_i^{\mathrm{c}},v_a\right)=\mathbf{0} \tag{11}$$

$$\mathbf{S}_2^{\mathrm{B}}(u_i,1)-\mathbf{S}^{\mathrm{M}}\left(u_i^{\mathrm{c}},v_b\right)=\mathbf{0} \tag{12}$$

$$\frac{\mathbf{S}_{1,u}^{\mathrm{B}}(u_i,0)\times\mathbf{S}_{1,v}^{\mathrm{B}}(u_i,0)}{\left\|\mathbf{S}_{1,u}^{\mathrm{B}}(u_i,0)\times\mathbf{S}_{1,v}^{\mathrm{B}}\left(u_i,0\right)\right\|}-\frac{\mathbf{S}_u^{\mathrm{M}}\left(u_i^{\mathrm{c}},v_a\right)\times\mathbf{S}_v^{\mathrm{M}}\left(u_i^{\mathrm{c}},v_a\right)}{\left\|\mathbf{S}_u^{\mathrm{M}}\left(u_i^{\mathrm{c}},v_a\right)\times\mathbf{S}_v^{\mathrm{M}}\left(u_i^{\mathrm{c}},v_a\right)\right\|}=\mathbf{0} \tag{13}$$

$$\frac{\mathbf{S}_{2,u}^{\mathrm{B}}(u_i,1)\times\mathbf{S}_{2,v}^{\mathrm{B}}(u_i,1)}{\left\|\mathbf{S}_{2,u}^{\mathrm{B}}(u_i,1)\times\mathbf{S}_{2,v}^{\mathrm{B}}\left(u_i,1\right)\right\|}-\frac{\mathbf{S}_u^{\mathrm{M}}\left(u_i^{\mathrm{c}},v_b\right)\times\mathbf{S}_v^{\mathrm{M}}\left(u_i^{\mathrm{c}},v_b\right)}{\left\|\mathbf{S}_u^{\mathrm{M}}\left(u_i^{\mathrm{c}},v_b\right)\times\mathbf{S}_v^{\mathrm{M}}\left(u_i^{\mathrm{c}},v_b\right)\right\|}=\mathbf{0} \tag{14}$$

$$u_i^{\mathrm{c}}=(u_i-u_a)\big/(u_b-u_a) \tag{15}$$

where u_i is the scatter parameter in range [0, 1] of the fitting surface $\mathbf{S}^{\mathrm{B}}(u,v)$, and u_i^{c} is the isoparametric of the machining

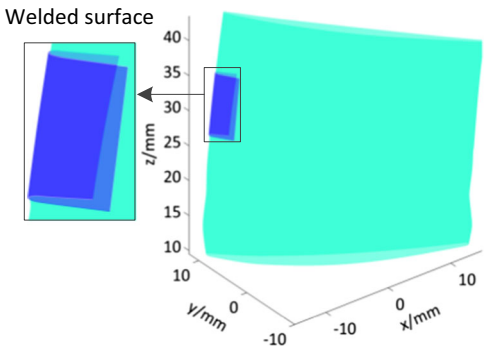

Fig. 9 Welded surface

Table 1 Optimized results of the curves of the repaired area (mm, mm, °)

No.	Control point 1 (Δx, Δy, θ)	Control point 2 (Δx, Δy, θ)	Control point 72 (Δx, Δy, θ)
Curve 1	(0.011, 0.021, 0.005)	(0.003, 0.032, 0.005)	(0.009, 0.023, 0.005)
Curve 2	(0.015, 0.015, 0.012)	(0.012, 0.018, 0.012)	(−0.014, 0.048, 0.012)
Curve 3	(0.010, 0.020, 0.008)	(0.006, 0.027, 0.008)	(0.010, 0.020, 0.008)
Curve 4	(0.010, 0.020, 0.007)	(0.008, 0.023, 0.007)	(−0.011, 0.043, 0.007)
Curve 5	(0.014, 0.020, 0.010)	(0.011, 0.023,0.010)	(0.016, 0.015, 0.010)

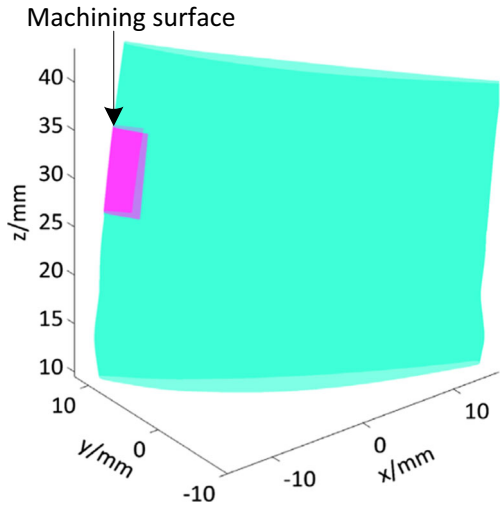

Fig. 10 The repaired target machining surface

surface $\mathbf{S}^{\mathrm{M}}(u,v)$. $\mathbf{S}_u^{\mathrm{B}}(u,v)$ and $\mathbf{S}_v^{\mathrm{B}}(u,v)$ are first tangent vector in the u direction and v direction on the surface $\mathbf{S}^{\mathrm{B}}(u,v)$. $\mathbf{S}_u^{\mathrm{M}}(u,v)$ and $\mathbf{S}_v^{\mathrm{M}}(u,v)$ are the first tangent vector in the u direction and v direction on the surface $\mathbf{S}^{\mathrm{M}}(u,v)$. The v_a, v_b, u_a, and u_b are the parameters of the regular repair area boundary on the surface $\mathbf{S}^{\mathrm{M}}(u,v)$ (Fig.7).

5.5 Concave-convex constraint

The shape of the cross-section curves for the blade has a great influence on the aerodynamic performance of the aircraft. Therefore, the inflection point is not allowed on the pressure surface or suction surface of the machining surface. All of control points, affect transition area of section curve segments, should be on one side of curve but not on each side. For suction side, the control points should be inside of machining section curve considering the section curve of the area is convex curve.

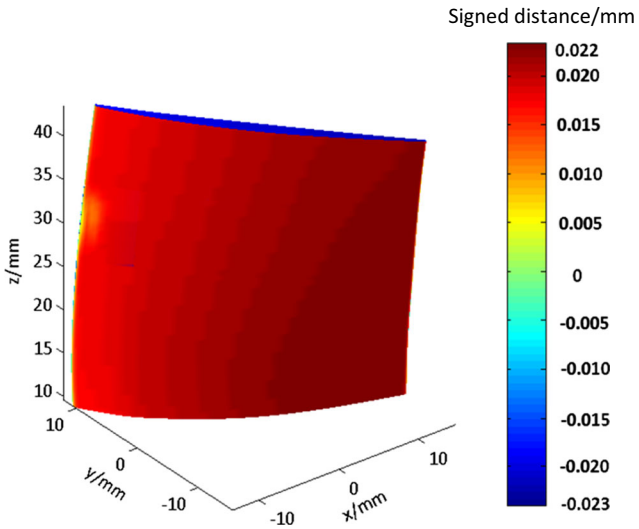

Fig. 11 Signed distance from the machining surface to the design surface

$$f_{convex} = (\mathbf{V}_i - P_i)\cdot\mathbf{n}_i \geq 0 \tag{16}$$

The judgment of concave-convex constraint is similar to the allowance constraint. The nearest points, corresponding to control points $\mathbf{V}_i$ of curves $\tilde{\mathbf{c}}_j^{\mathrm{D}}(u)$, are P_i on machining section curve, and $\mathbf{n}_i$ is the outer normal vector at points P_i.

For pressure side, the control points should be outside of section curve $\tilde{\mathbf{c}}_j^{\mathrm{D}}(u)$ of the machining surface, since the section curves of the area is concave curve.

$$f_{concave} = (\mathbf{V}_i - P_i)\cdot\mathbf{n}_i \leq 0 \tag{17}$$

6 Simulation results and discussion

A compressor blade is taken as an instance to verify the above method. The profile tolerance of design surface is ±0.05 mm. After machining datum matching with design datum, the worn area is determined based on blade inspection results (Fig. 8a). Then, a pre-inspection process is performed to judge whether the deviation between the measured points of the service blade and the design surface is within the tolerance. It can be seen from Fig. 8b, the max sign distance is 0.021 mm, which indicates that worn blade can be repaired.

Then, the worn area is cut into a regular area, and the parameter range $u = [0.46, 0.6] v = [0.25, 0.5]$ of regular area is determined. Five intersection curves between upper profile tolerance surface $\mathbf{S}^{\mathrm{U}}(u,v)$ and planes $\{H_1, H_2, \cdots, H_n\}$ are obtained at$H_1 = 34.500$, $H_2 = 32.264$, $H_3 = 30.021$, $H_4 = 27.768$, and $H_5 = 25.500$ mm by Newton iterative method. The curve segment corresponding to parameter range [0.46, 0.6] is split to construct welded surface (Fig. 9).

Limited by the welding process, the welded blade needs to be machined subsequently. In order to reduce the influence of clamping deformation for the accuracy of the target machining surface, an on-machine measurement technology for welded blade is used to compensate clamp error. An accurate machining surface can be found out with the proposed optimization model. There are 72 control points for each section curve. Table 1 lists the optimized results of the five strip profile curves displacement. The optimized machining surface is presented in Fig. 10.

In order to judge the repaired machining surface is whether within the allowance profile tolerance zone. Two thousand five hundred points are sampled on the machining surface, then the signed distance between the sampling points and the nearest points of the design surface is calculated (Fig. 11). The maximum absolute value of the signed distance is 0.023 mm. Therefore, optimized machining surface satisfies the design requirements.

The boundary geometric continuities between the machining surface and the unrepaired area are shown in Fig. 12.

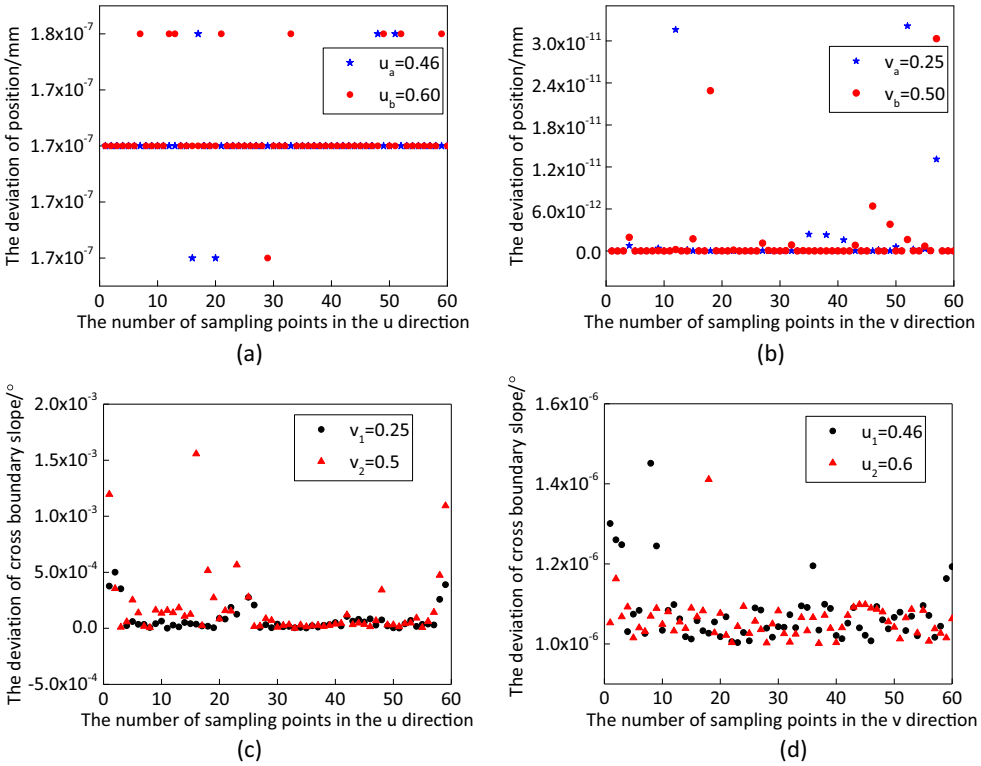

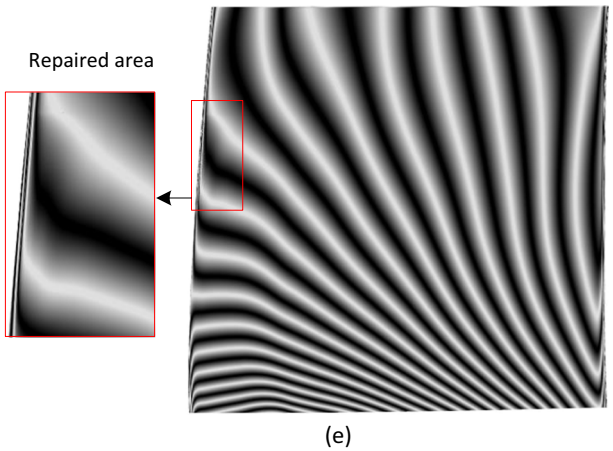

Fig. 12 Geometric continuity between the machining surface and undamaged area. **a** G^0 continuity in the *u* direction. **b** G^0 continuity in the *v* direction. **c** G^1 continuity in the *u* direction. **d** G^1 continuity in the *v* direction. **e** G^2 continuity

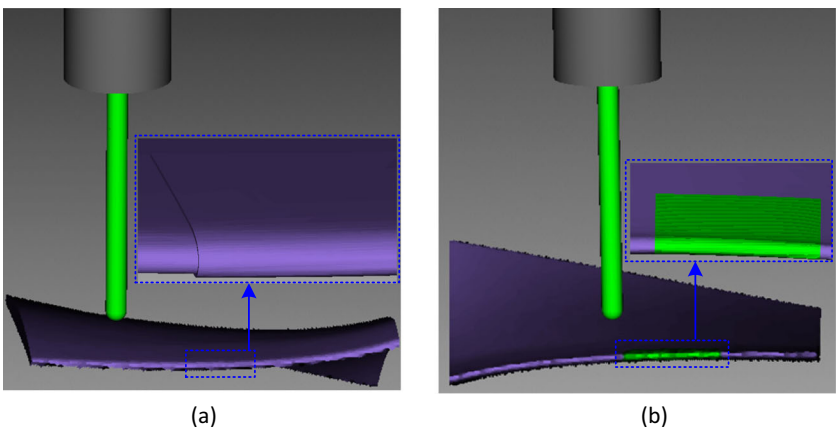

Fig. 13 Simulation results in VERICUT software. **a** Welded model. **b** The machined blade model

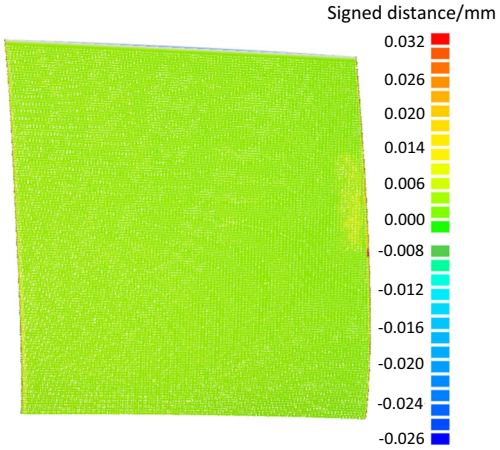

Fig. 14 Signed distance between the cutting model and the design surface

Figure 12a, b is the position deviation on the parameter *u* direction and *v* direction. The max positional deviations (G^0) are 1.8×10^{-7} mm in the *u* direction and 3.12×10^{-7} mm in the *v* direction. The max tangent deviation (G^1) in the *u* direction and *v* direction is 0.0015° and 1.4×10^{-6}°, respectively (Fig. 12c, d). The *G*2 continuity along the *u* direction between machining surface and rest blade area is checked by zebra stripes (Fig. 12e). The results indicate that the optimized machining surface satisfies geometric continuities.

In order to verify whether the blade after machining can meet the accuracy requirements, a 5-axis machining strategy is used to remove excess material effectively in VERICUT software (Fig. 13a). The welded blade imported the VERICUT software in IGES format, which is the blank of finishing machining. In addition, machining datum, machining tool, cutting parameter, and planning of tool path have been well considered. However, it is unavoidable for clamp deformation in machining process may cause inaccurate geometric model. For the adaptive repair process, it can be solved by measuring the welded blade while it has been clamped, which can compensate the error caused by the clamping deformation. The blade after machining is in Fig. 13b.

The blade after machining in the VERICUT software and its design surface are exported to reverse engineering software in STL format. As it can be seen, the maximum signed distance from the repaired surface to the design surface is 0.032 mm (Fig. 14). Simulation results show that the proposed approach is feasible for repairing complex blade surface.

7 Conclusion

Aero engine blade repair is a challenging issue due to the deformation caused by excessive work leading to the unknown target machining surface during repair process. Therefore, it is important for aerospace industries to repair worn blades with an automated, accurate, reliable, and fast solution. Current repair methods mainly rely on some commercial reverse engineering software to obtain the machining surface artificially. The tolerance requirements and geometric continuity are not guaranteed accurately. Thus, to avoid a massive manual intervention, an adaptive blade repair approach is proposed in this paper.

The method integrates restructuring welded surface and machining surface and adapts to the undamaged part based on the measured model through the coordinate measuring machine. These created surfaces can be utilized in CAM system for tool path generation in welded process and machining process. Compared with the present methods of blade repair, the advantages of the proposed approach are the following: (1) enough material is left for subsequent machining during welded surface modeling. (2) For near-net allowance welded workpiece, the machining surface restructured adapts to the undamaged area and satisfies the design requirements. (3) The high-accuracy machining surface created with an effective optimization method can compensate the clamping error, in addition, and is also found out automatically.

Acknowledgements The project was supported by the Natural Science Basic Research Plan in Shaanxi Province of China (2016JM5040).

Compliance with ethical standards

Conflict of interests The authors declare that they have no conflict of interest.

References

1. Huang X, Miglietti W (2012) Wide gap braze repair of gas turbine blades and vanes—a review. Journal of Engineering for Gas Turbines & Power 134(1):010801
2. Schlobohm J, Bruchwald O, Frackowiak W, Li Y, Kästner M, Pösch A, Reimche W, Reithmeier E, Maier HJ (2016) Turbine blade wear and damage—an overview of advanced charact. Materialprufung 58(5):389–394
3. Sheng X, Kromker M (1998) Surface reconstruction and extrapolation from multiple range images for automatic turbine blades repair. Industrial Electronics Society, 1998. IECON '98. Proceedings of the, Conference of the IEEE 1315-1320 vol.3
4. Chen Q, Sun Z, Zhang W, Gui Z (2008) A robot for welding repair of hydraulic turbine blade. Robotics, Automation and Mechatronics, 2008 I.E. Conference on. IEEE 155–159
5. Mohaghegh K, Sadeghi MH, Abdullah A (2007) Reverse engineering of turbine blades based on design intent. Int J Adv Manuf Technol 32(9):1009–1020
6. Cripps D (2011) The future of blade repair. Reinf Plast 55(1):28–32
7. Bremer C (2000) Adaptive strategies for manufacturing and repair of blades and blisks. ASME Turbo Expo 2000: Power for Land, Sea, and Air V004T01A010-V004T01A010
8. Huang H, Zhou L, Chen XQ, Gong ZM (2003) SMART robotic system for 3D profile turbine vane airfoil repair. Int J Adv Manuf Technol 21(4):275–283

9. Huang H, Gong ZM, Chen XQ, Zhou L (2002) Robotic grinding and polishing for turbine-vane overhaul. J Mater Process Technol 127(2):140–145
10. Zheng J, Li Z, Chen X (2006) Worn area modeling for automating the repair of turbine blades. Int J Adv Manuf Technol 29(9):1062–1067
11. Brinksmeier E, Berger U, Janssen R (1998) Advanced mechatronic technology for turbine blades maintenance. Power Station Maintenance - Profitability Through Reliability. First Iee/imeche International Conference on IET 184-189
12. Ng TJ, Lin WJ, Chen X, Gong Z (2005) Intelligent system for turbine blade overhaul using robust profile re-construction algorithm. Control, Automation, Robotics and Vision Conference, 2004. Icarcv 2004. IEEE Xplore 178-183 Vol. 1
13. Anonymous (2004) Aerofoil machining and polishing combined into a single automated process. Aircr Eng Aerosp Technol An Int J 76(5):542–543
14. Bremer C (2005) Automated Repair and Overhaul of Aero-Engine and Industrial Gas Turbine Components. ASME Turbo Expo 2005: Power for Land, Sea, and Air 841–846
15. He J, Li L, Li J (2011) Research of key-technique on automatic repair system of plane blade welding. International Conference on Control, Automation and Systems Engineering. IEEE 1-4
16. Yilmaz O, Gindy N, Gao J (2010) A repair and overhaul methodology for aeroengine components. Robot Comput Integr Manuf 26(2):190–201
17. Gao J, Folkes J, Yilmaz O et al (2005) Investigation of a 3D non-contact measurement based blade repair integration system. Aircr Eng Aerosp Technol 77(1):34–41
18. Gao J, Chen X, Zheng D et al (2006) Adaptive restoration of complex geometry parts through reverse engineering application. Adv Eng Softw 37(9):592–600
19. Gao J, Chen X, Yilmaz O, Gindy N (2008) An integrated adaptive repair solution for complex aerospace components through geometry reconstruction. Int J Adv Manuf Technol 36(11):1170–1179
20. Wu H, Gao J, Li S, Zhang Y, Zheng D (2013) A review of geometric reconstruction algorithm and repairing methodologies for gas turbine components. Telkomnika Indones J Electr Eng 11(3)
21. Yilmaz O, Gindy N, Gao J (2010) A repair and overhaul methodology for aeroengine components. Robot Comput Integr Manuf 26(2):190–201
22. Zhang Y, Zhang D, Wu B (2010) A geometry reconstruction approach based on cross-section curve blending for adaptive repair of blades. ICRM- Green Manufacturing 146–151
23. PIEGL L, TILLER W (1997) The NURBS book, 2nd edn **Springer-Verlag New York**
24. Chun C (2005) Iterative methods improving Newton's method by the decomposition method *[J]. Comput Math Appl 50(10):1559–1568
25. Patrikalakis NM, Maekawa T (2010) Shape Interrogation for Computer Aided Design and Manufacturing[M]. Springer, Berlin Heidelberg